Chapter 7

Antiproton mass measurement and other experiments in an ion trap

7.1 Antiproton mass measurement

7.1.1 Antiproton cyclotron frequency measurement

Comparison of antiproton and proton cyclotron frequencies yields the ratio of inertial masses [12,25]

$$m(\overline{p})/m(p) = 0.999\ 999\ 977(42). \tag{7.1}$$

Antiprotons are cooled into the harmonic potential well by a cloud of electrons. Then most electrons are removed from the trap by suddenly reducing the trapping potential to 4 V or less while applying a strong axial drive ν_z(e) and axial cooling sideband drive ν_z(e)+ν_m(e). When the antiprotons are driven very close to their cyclotron sideband frequency $\nu_c' + \nu_m$ for a short period and enough energy is pumped into their axial motion and cyclotron motion, the heating signals are detected from the axial preamplifier and cyclotron preamplifier simultaneously.

These signals are directly shown on two spectrum analyzers after further amplification.

If too much energy is put into the system, signals are broadened. Especially the cyclotron signal is asymmetric. While antiprotons dissipate energy via electron cooling and resistor damping, the linewidth becomes narrower and the cyclotron ν_c' signal becomes more symmetric. The damping time ranges from a few seconds to hours. We can deduce the cyclotron frequency ν_c from the invariance theorem [81]

$$(\nu_c)^2 = (\nu_c')^2 + (\nu_z)^2 + (\nu_m)^2 \tag{7.2}$$

which has been shown to be invariant under the leading perturbations of an imperfect Penning trap. The magnetron frequency can be eliminated from the invariance theorem to obtain the approximation

$$\nu_c \approx \nu_c' + \nu_z^2/2\nu_c'. \tag{7.3}$$

The higher order terms are negligible, and will be discussed later. Antiprotons are confined in the center of the ring which is split into 4 segments. The cyclotron frequency drive line is connected to two ring segments. The third segment is used for cyclotron frequency detection and the other provides an RF ground. The amplified cyclotron signal is mixed down below 100 kHz and can be observed on a spectrum analyzer (HP 3561A Dynamic Signal Analyzer). The amplified axial signal from the lower compensation electrode can be seen from an HP 8562A spectrum analyzer with a lower resolution (minimum resolution bandwidth 100 Hz). The schematic diagram for antiproton (proton) cyclotron frequency measurement is shown in Fig. 7.1. In our system, a 50 Hz shift in axial frequency corresponds to 1 Hz modification to the cyclotron frequency. Typical resonant signals for the antiproton cyclotron frequency measurement are shown in Fig. 7.2. In Fig. 7.2(a), the antiproton cyclotron frequency ν_c' = 89 133 083±1 Hz with a width of 2 Hz is plotted. Fig. 7.2(b) shows the antiproton axial resonance. The axial frequency is

ν_z = 1 907 550±100 Hz and hence the magnetron frequency ν_m=20 412±2 Hz is obtained. Therefore we have $\nu_c = \nu_c' + \nu_m$ = 89 153 495±2 Hz.

Proton cyclotron measurements are carried out in the same way except the polarity of the trapping potential is opposite. The electron cyclotron frequency is obtained when a microwave drive is swept through the cyclotron which shifts the electron axial. Thereby the mass ratios of antiproton to proton, antiproton to electron, and proton to electron are measured. Averaging over 5 comparisons [12], we obtain $m(\overline{p})/m(p) = 0.999\ 999\ 977$. Antiproton and proton masses are in agreement within an uncertainty of 4×10^{-8}. The mass ratio of proton to electron [12] is in good agreement with a slightly more accurate m_p/m_e value [23].

7.1.2 Systematic analysis and results

Even though the linewidth of the observed signals can be very narrow with a resolution of 10^{-8}, systematic effects may cause much larger shifts due to trap imperfections, field inhomogeneity, and particle interactions. The long term drift of the superconducting magnet must be accounted for. Small magnetic field fluctuations are shielded [55] while large magnetic field shifts need special corrections.

It is necessary to examine the validity of the simple formula we have used in the equation $\nu_c = \nu_c' + \nu_z^2/2\nu_c'$. Considering the effects of misalignments of the magnetic field to the axis of the electric quadrupole following Ref. [73]:

$$\mathbf{B} = B(cos\theta\mathbf{i} + sin\theta cos\phi\mathbf{j} + sin\theta sin\phi\mathbf{k}) \tag{7.4}$$

and internal misalignments of the trap electrodes causing departure of the quadratic terms in the electrostatic potential:

$$U = (1/2)m\omega_z^2[z^2 - (1/2)(x^2 + y^2) - (1/2)\varepsilon(x^2 - y^2)] \tag{7.5}$$

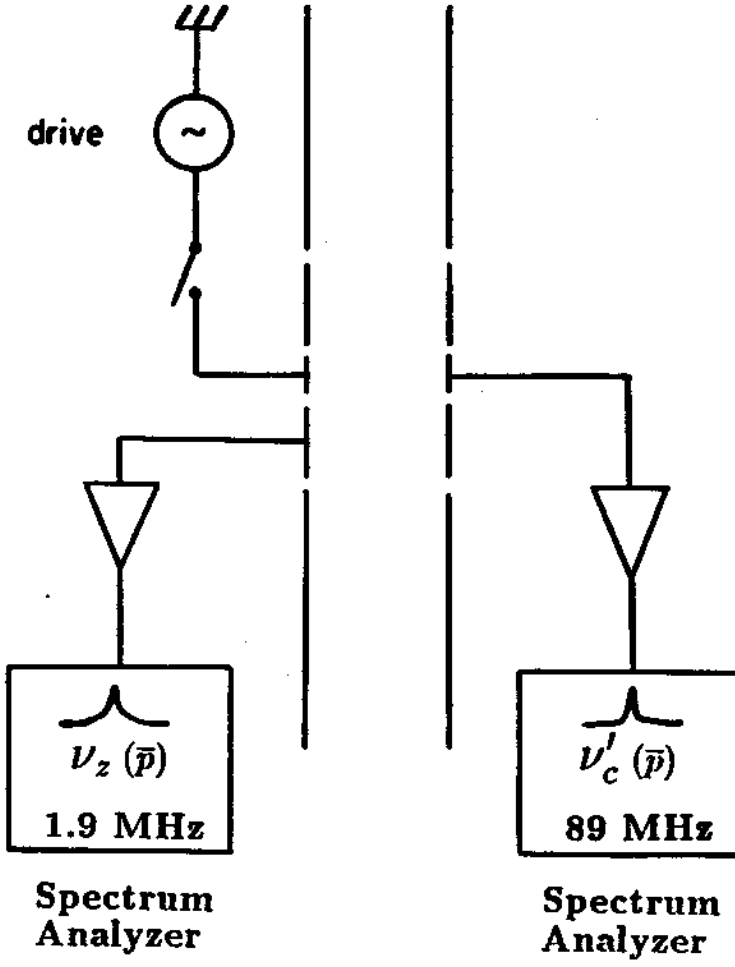

Figure 7.1: Schematic diagram for antiproton (proton) cyclotron frequency measurement.

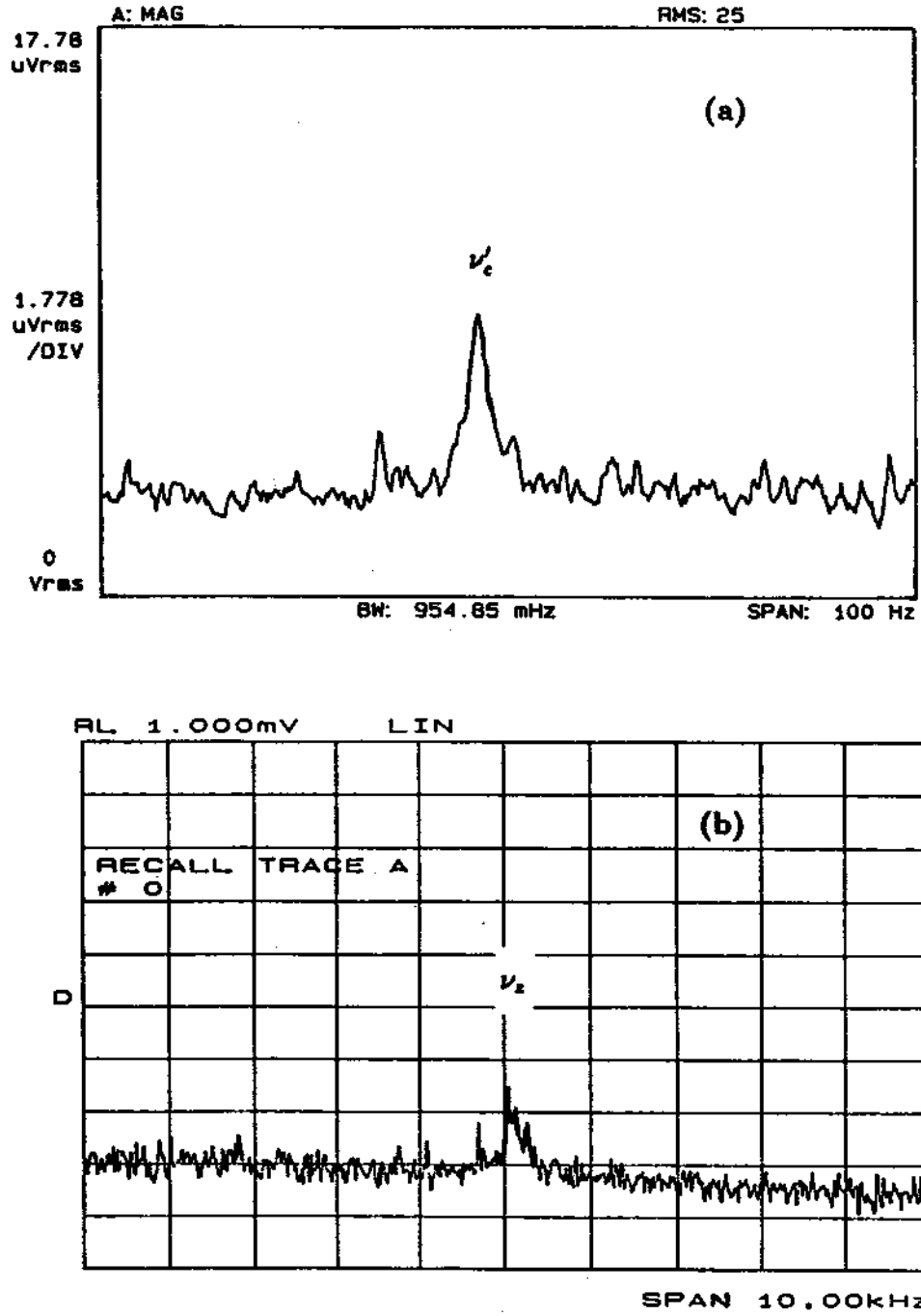

Figure 7.2: (a) Antiproton cyclotron resonance. (b) Antiproton axial resonance.

where ϵ is the asymmetry parameter representing the harmonic imperfections. The fractional correction to the above electromagnetic static fields is given by

$$\Delta\nu_c/\nu_c \approx (9/16)(\nu_z^4/\nu_c'^4)(\theta^2 - 2\epsilon^2/9) \tag{7.6}$$

For electrons with an axial frequency of 54 MHz and a cyclotron frequency of 164 GHz, we have

$$\Delta\nu_c/\nu_c(\theta = 1^o, \epsilon = 0) = 2 \times 10^{-18}, \tag{7.7}$$

and

$$\Delta\nu_c/\nu_c(\theta = 0, \epsilon = 0.01) = -1.5 \times 10^{-19}. \tag{7.8}$$

For proton (antiproton) frequencies of $\nu_z = 1.91$ MHz and $\nu_c' = 89.3$ MHz, the corrections from Eqs. (7.7) and (7.8) are 3.6×10^{-11} and -2.6×10^{-12}, respectively.

There are many sources such as gaps in the electrodes, machining error in electrode dimensions, and misaligned trap which can introduce trap anharmonicity. The most significant anharmonicity is from the C_4 term which was introduced in Chapter 5. The shift in the cyclotron frequency measurement is given as [73]

$$\Delta\nu_c/\nu_c \approx (3/4)C_4(\nu_z/\nu_c)^2(\rho_m/z_0)^2. \tag{7.9}$$

It depends on the location of the particles. A large magnetron orbit will make a big shift. For example, we have $(\nu_z/\nu_c)^2 = 1.1 \times 10^{-7}$ for electron and 4.6×10^{-4} for proton (antiproton) in our system. We take $\rho_m/z_0 = 0.1$, that is, $\rho_m \approx 0.6$ mm, then the effects are

$$\Delta\nu_c/\nu_c = 3.5 \times 10^{-6} C_4 \ for\ antiproton, \tag{7.10}$$

and

$$\Delta\nu_c/\nu_c \approx 10^{-8} C_4 \ for\ electron. \tag{7.11}$$

Since $C_4 < 10^{-3}$ (it can be tuned away by adjusting the compensation potential V_c. The C_4 given here corresponds $\Delta V_c = 0.1$ V), this effect only contributes a small

shift for antiprotons which is less than 10^{-8}, and is negligible for an electron. This has been tested experimentally by searching for frequency shifts while changing the compensation potential.

A magnetic field homogeneity of $10^{-8}/cm^3$ can be achieved in our magnet as measured with NMR techniques without the presence of the trap. Once the center of the magnet is surrounded by trap electrodes, the field is distorted by the paramagnetism and diamagnetism of the trap material. The magnetizations for Cu is -0.05 and for MACOR is $+0.78$ (see Ref. [73]). The lowest order axial component of the magnetic field can be expressed as

$$\Delta B_z = B_z(z^2 - \rho^2/2). \tag{7.12}$$

This magnetic bottle causes a cyclotron frequency shift of

$$\Delta\nu_c/\nu_c = B_2(z^2 - \rho_m^2). \tag{7.13}$$

The coefficient B_2 is calculated to be less than $10^{-7}/mm^2$. The effect is less than 2×10^{-8} for z = 0 and $\rho_m = 0.4$ mm.

For a cloud of charged particles of a single species, no frequency shifts should be observed since only center-of-mass motions of the cloud are detected by the preamplifiers [66]. There is no number dependency observed at the 10^{-8} level. The possible effect from the contaminant particles are studied. For typical cloud densities and compositions used, we conclude that the effect of contaminant particles are less than 2×10^{-8}.

Using half the observed cyclotron linewidth as the uncertainty, the fractional standard deviation of the five measured ratios is 3.4×10^{-8}, while the scatter in the five independent sets of comparisons is only 1.4×10^{-8}. We obtained the error quoted by adding the standard deviation for the point, the scatter, and the

systematic limit in quadrature, to obtain a standard deviation which is 4.2×10^{-8} of the mass ratio. The new mass ratio of antiproton and proton

$$m(\overline{p})/m(p) = 0.999\ 999\ 977(42) \tag{7.14}$$

is shown in Fig. 7.3, comparing with previous measurements. The error bar for our measurement is 50 times smaller than the diameter of the point. The fractional uncertainty of 4×10^{-8} is 1000 times more accurate than previous antiproton mass measurements using exotic atoms and is the most precise test of CPT invariance with baryons.

7.2 The gravitational mass of antimatter

The gravitational mass of the antimatter has not yet been directly measured. So far, there is no successful quantum field theory for gravitational fields to anticipate it and to explicitly establish CPT invariance. To measure the gravitational acceleration of the antiproton by launching ultracold antiprotons up through a 1 meter long (L) vertical drift tube from a Penning trap has been proposed [82]. The plan is to use the time of flight technique similar to the reported measurement of the electron gravitational force by Witteborn and Fairbank [83]. A cutoff time ($t_c = \sqrt{2L/g}$) will be measured for the lowest energy antiprotons reaching a detector at the top of the drift tube, hence the gravitational acceleration g is obtained. The cutoff time would be 0.45 sec for an initial kinetic energy of 0.1 μV which is required to overcome the 1 m height difference if we assume $g(\overline{p}) = g(p)$. This is a direct test of the equality of particle and antiparticle gravitational masses with protons and antiprotons. They propose to achieve a 1% accuracy measurement of the gravitational acceleration of antiprotons relative to the H^- ion by launching of a total of 10^6 to 10^7 particles. However, the major difficulties arise from the extreme weakness of the gravitational interaction. Even a single charged particle

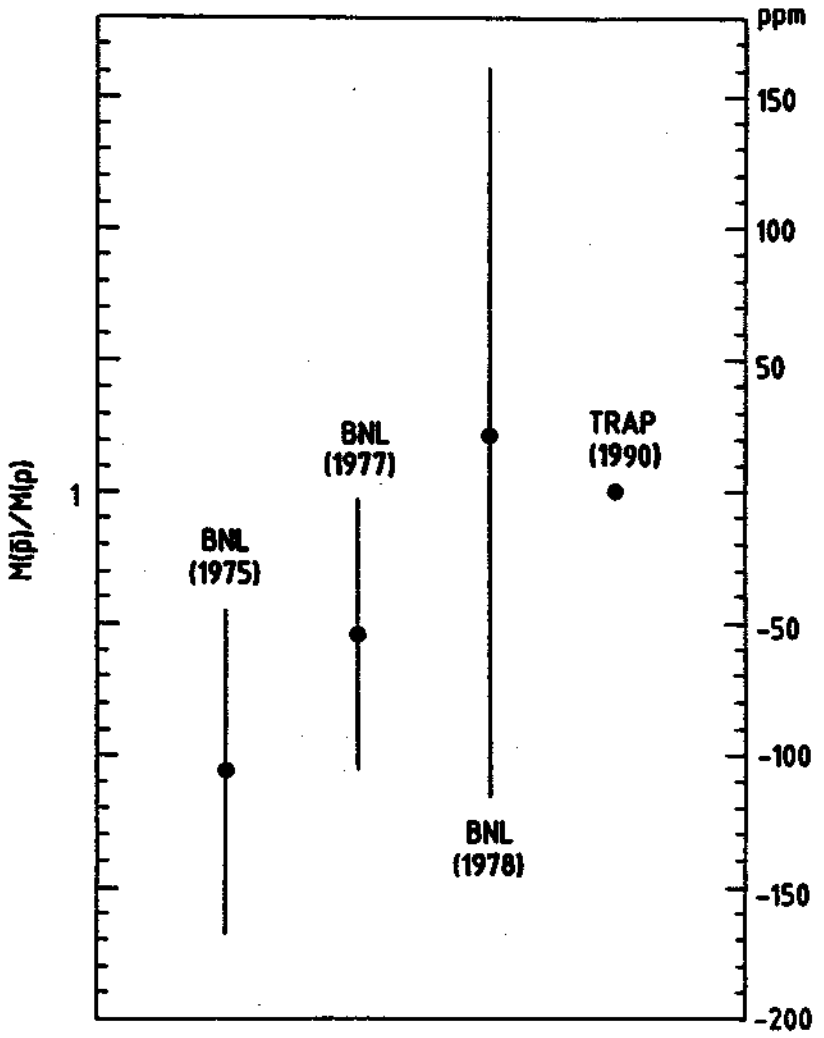

Figure 7.3: The new mass ratio of antiproton and proton is shown here, comparing with previous measurements. The error bar for our measurement is 50 times smaller than the diameter of the point.

within 12 cm would be able to balance the gravitational force of the earth acting on an antiproton if we assume that an antiproton has the same gravitational mass as the proton. Since antihydrogen is less sensitive to stray electric fields, a gravitational measurement of antihydrogen seems more promising once it is available [6]. The strong Coulomb repulsion between the particles as they are launched also can cause large problems. Such Coulomb explosions and stray fields in our apparatus have limited our energy resolution to 5 meV, while the gravitational potential energy for a proton over one meter is 10^{-4} meV.

7.3 Antihydrogen production and antihydrogen physics

A positron and an antiproton together will form an antihydrogen atom. If low energy positrons and antiprotons can interact with each other in a nested trap as discussed in Ref. [7] which consists a series of electrodes, antihydrogen would be produced [7]. In this scheme, preloaded positrons from a positron moderator are confined in a harmonic potential well with negative potentials on the ring and compensation electrodes. By positron cooling which is analogous to the electron cooling described in Chapter 5, antiprotons trapped in the long trap lose energy while colliding with positrons. Since the potential well for positrons is a potential barrier for antiprotons, only antiprotons with a kinetic energy larger than the effective barrier potential energy can interact with positrons and have a chance of forming antihydrogen. During the antiproton slowing process the recombination rate is enhanced greatly since the reaction rate is higher when the relative velocity between positron and antiproton is lower. Two processes would happen naturally: radiative recombination $\overline{p} + e^+ \longrightarrow \overline{H} + h\nu$, and 3-body recombination $\overline{p} + e^+ + e^+ \longrightarrow \overline{H} + e^+$. The 3 body recombination process could give very high production rate at low temperature (about 600 per second per antiproton for a

positron density of $10^7/cm^3$ at 4.2 K) [5] since the rate-temperature dependence is $T^{-9/2}$ while radiative recombination is $T^{-1/2}$.

Other proposed methods are merging a positron beam or positronium beam with antiprotons $Ps + \overline{p} \longrightarrow \overline{H} + e^-$ [3]. Antihydrogen physics may include precision antihydrogen spectroscopy, antihydrogen gravitational mass measurement [6], and the formation of antihydrogen molecules. Other ideas can be found in Ref.[3].

7.4 Antideuteron

Trapping antiprotons and related studies can be naturally applied in trapping heavier charged antinuclei such as an antideuteron. Conservation of baryon number requires that antiprotons and antideuterons can only be produced along with their particle counterparts:

$$p + p \longrightarrow p + p + \overline{p} + p, \tag{7.15}$$

and

$$p + p \longrightarrow p + p + \overline{d} + d. \tag{7.16}$$

The initial proton energy needed to produce one antinucleus must have a net center of mass energy of twice the nucleus mass. For antiprotons produced when fast protons collide with protons at rest, the laboratory energy of the incident protons must be above 5.6 GeV. Actually the Berkeley Bevatron was designed at 6 GeV to exceed this threshold energy for antiproton production. However, if the target proton is in a Cu-nucleus, it is a moving target because it undergoes Fermi motion. Antiprotons can thus be produced with 3 GeV protons incident on targets containing heavy elements, but with much lower production rates since only a small fraction of collisions are head on collisions with the moving target protons. The higher the incident proton energy, the more the antiparticle yield per proton. Due to the proton beam energy requirement, it is much more difficult to make heavier

antiparticles. Antideuteron was discovered in 30 GeV proton-beryllium collisions at BNL [84]. With 30 GeV protons incident upon protons at rest, the net energy available is 5.74 GeV which is larger than $2m_{\overline{d}} \approx 4$ GeV. Production of fairly large amounts of antideuteron is feasible. The possibility of building an antideuteron ring similar to LEAR has been discussed [85]. Many fewer antideuterons would be accumulated compared with antiprotons since heavier particles are more difficult to produce. Koch estimated the $\overline{d}/\overline{p}$ ratio for a 26 GeV/c primary, 3.5 GeV/c secondary, in the forward direction to be 4×10^{-6} $\overline{d}/\overline{p}$. This gives 200 $\overline{d}$ per pulse (10^{13} p) in a storage ring. With small modifications to the present antiproton production facility at CERN more than 10^6 antideuterons per day could be stored and used for experiments [86]. If those stored antideuterons could be decelerated to the order of 10 MeV, it seems possible to trap and cool a few antideuterons in an ion trap. The antideuteron energy loss (dE/dx) in matter is the same as for antiprotons of same velocity. Their energy stragglings in matter are very similar. For example, the 12 MeV antideuteron straggling parameter in Al is 1.4 times that of 6 MeV antiprotons [37]. The low energy antideuteron yield should be more than 10^{-4}/keV for the 12 MeV beam based on the antiproton test. Therefore, 10^2 antideuterons per day could be confined in an ion trap if we assume the slowing and trapping efficiency is 10^{-4} which has been achieved in our antiproton experiment. The particles in the trap are suitable for the high precision antideuteron mass measurement, and thus the antineutron mass and the binding energy in antideuteron (the binding energy for deuteron is 2.225 MeV).

7.5 Portable antiproton source

The movable source of antiprotons could make antiprotons available to a new research community normally unrelated to the accelerator physics. Portable antiprotons stored in an ion trap and transferred between laboratories has been

suggested [87]. One big concern is that a very good vacuum is needed to eliminate antiproton loss by collisions with neutral gases. The long lifetime of the antiprotons in an ion trap demonstrated in this experiment shows that the particle loss could be insignificant during long shipping and waiting periods of several months.

7.6 Summary

Summarizing, energetic antiprotons are slowed down in matter and captured indefinitely in an ion trap. They reach thermal equilibrium with their surroundings at 4.2 K via electron cooling or resistor damping. High precision mass comparisons for antiproton and proton (or electron) in the trap are carried out with a fractional accuracy of 4×10^{-8} which is a 1000-fold improvement in the measured antiproton mass. Another factor of 100 improvement is sought. Trapped cryogenic antiprotons are also suited for antiproton-atom interaction studies, antihydrogen production, antimatter gravitational mass measurements, long time storage and transfer. The great success of trapping low energy antiprotons in an ion trap marks the completion of the task of confining all the stable charged elementary particles (electrons, positrons, protons and antiprotons) and opens the way to other intriguing experiments.